Asymmetric Diketopyrrolopyrrole Conjugated Polymers for Field-Effect Transistors and Polymer Solar Cells Processed from a Nonchlorinated Solvent

Yunjing Ji, Chengyi Xiao, Qiang Wang, Jianqi Zhang, Cheng Li, Yonggang Wu, Zhixiang Wei, Xiaowei Zhan, Wenping Hu, Zhaohui Wang, René A. J. Janssen,* and Weiwei Li**

Conjugated polymers based on electron-deficient diketopyrrolopyrrole (DPP) units have been intensively explored and applied in solution-processed organic electronic devices. Due to their good planarity and strong intermolecular π–π interactions of the conjugated backbone, DPP polymers show high carrier mobilities > 1 $cm^2\ V^{-1}\ s^{-1}$ in field-effect transistors (FETs),[1–8] exceeding those of amorphous silicon. The strong electron-withdrawing character of DPP units also causes DPP polymers to absorb near infrared light and their absorption spectra cover a significant part of the solar spectrum. As a result, DPP-based polymer solar cells (PSCs) can provide high photocurrents above 20 mA cm^{-2}[9–11] and achieve excellent power conversion efficiencies (PCEs) > 8%.[11–13] Compared to other high-performance polymer semiconductors, DPP polymers show significantly less synthetic complexity.[14] All these merits indicate that DPP polymers have great potential for large-area industrial application. However, an important drawback of DPP polymers for FETs and PSCs is that the film formation requires the use of a chlorinated solvent, such as chloroform ($CHCl_3$), chlorobenzene, or *ortho*-dichlorobenzene (*o*-DCB), resulting in detrimental effects on the environment. Therefore, it is urgent to design new DPP polymers that can be solution-processed from nonchlorinated solvents for organic electronic thin film devices.

The repeat unit of DPP polymers generally comprises four different principal components: the DPP unit, flanked by two adjacent aromatic substituents, a central π-conjugated segment, and solubilizing alkyl chains on the lactam ring. The aromatic substituents originate from the aromatic nitrile precursors that are used to synthesize the DPP core, which does not exist as a unit by itself.[15] The solubility of the polymers is determined by their chemical structure in which the length of the side chains[16–18] and the size of conjugated segment are important parameters.[19] Long branched alkyl chains attached to the lactam ring of DPP enhance the solubility of the conjugated polymer and decrease the π–π stacking, promoting the hole mobilities in FETs.[7] However, the change of side chain length has little influence on the polarity and noncovalent interactions of the polymer backbone that prevent the polymer to become soluble in less-polar solvents, such as toluene. Furthermore, DPP polymers with long alkyl side chains were found to form a fibrillar micro-phase separation with large diameter fibrils in bulk-heterojunction solar cells, which lowers the efficiency for charge generation and the PCE.[16] However, the solubility of DPP polymers can be effectively adjusted by variations in the conjugated backbone. When the DPP monomers were randomly copolymerized with two different conjugated segments[20,21] or with an asymmetric conjugated segment,[22] the resulting DPP polymer lacks perfect translational symmetry along the chain and becomes well soluble in nonchlorinated solvents, such as toluene and tetrahydrofuran, while still affording high hole mobilities >1 $cm^2\ V^{-1}\ s^{-1}$ in FETs.

Here we focus on exploring new DPP polymers that can be solution-processed from nonchlorinated solvents for high-performance FETs and PSCs. Our design strategy is based on the use of two different flanking aromatic substituents on the DPP monomer. For the synthesis of symmetrical DPP monomers, the two aromatic units, such as benzene,[23,34] pyridine,[3,25,26] thiophene (T),[27,28] furan,[16,29,30] 3-methylthiophene (MT),[31] thieno[3,2-*b*]thiophene (TT),[12,32] selenophene,[33] and thiazole,[34,35] are introduced using their nitrile derivatives via one-step reaction with diethyl succinate. By using two-step methods, asymmetric DPP monomers can be synthesized, affording structures like T-DPP-MT or T-DPP-TT (**Scheme 1**). Asymmetric DPP compounds have also been reported for dye-sensitized solar cells.[36,37] In this work, we show the first example of asymmetric DPP polymers by incorporating two different aromatic substituents. The new DPP

Y. Ji, C. Xiao, Dr. C. Li, Prof. W. Hu,
Prof. Z. Wang, Prof. W. Li
Beijing National Laboratory for Molecular Sciences
Key Laboratory of Organic Solids
Institute of Chemistry
Chinese Academy of Sciences (ICCAS)
Beijing 100190, P.R. China
E-mail: licheng1987@iccas.ac.cn; liweiwei@iccas.ac.cn
Q. Wang, Prof. R. A. J. Janssen
Molecular Materials and Nanosystems
Eindhoven University of Technology
P.O. Box 513, 5600 MB Eindhoven, The Netherlands
E-mail: r.a.j.janssen@tue.nl
Dr. J. Zhang, Prof. Z. Wei
National Center for Nanoscience and Technology
Beijing 100190, China
Y. Ji, Prof. Y. Wu
College of Chemistry and Environmental Science
Hebei University
Baoding 071002, China
Prof. X. Zhan
Department of Materials Science and Engineering
College of Engineering
Peking University
Beijing 100871, China

DOI: 10.1002/adma.201504272

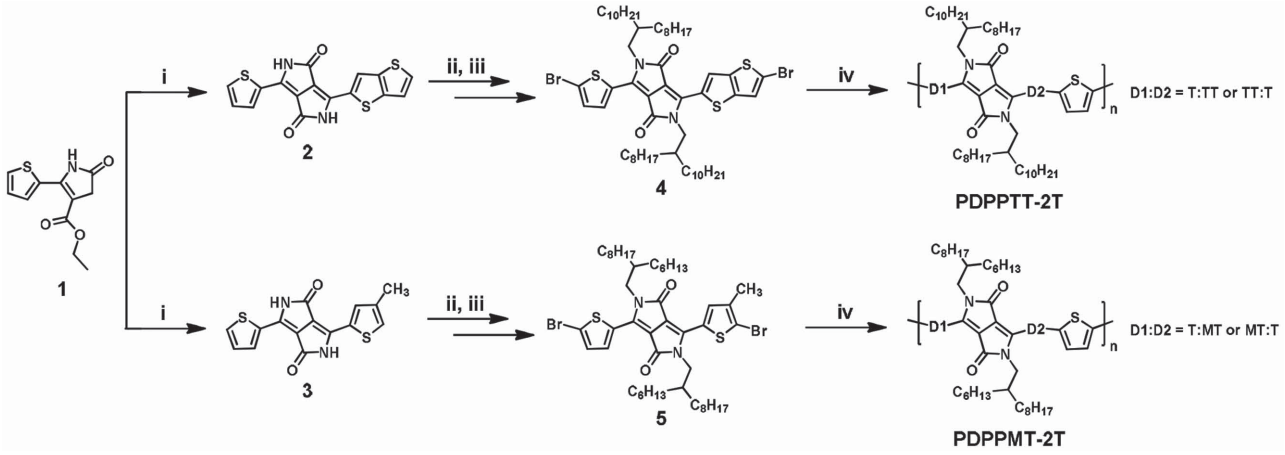

Scheme 1. Chemical structures of the DPP polymers PDPPTT-2T and PDPPMT-2T and their synthetic routes. T, thiophene; TT, thieno[3,2-*b*]thiophene; and MT, methylthiophene. i) sodium/$FeCl_3$ in 2-methyl-2-butanol at 95 °C, 2 h; **1** was added and thieno[3,2-*b*]thiophene-2-carbonitrile (or 4-methylthiophene-2-carbonitrile) was added dropwise at 120 °C; reflux at 120 °C, 3 h; ii) K_2CO_3, 18-crown-6, and 2-octyldodecyl bromide (or 2-hexyldecyl bromide) in DMF at 120 °C, 16 h; iii) Br_2 in $CHCl_3$; iv) Stille polymerization by using $Pd_2(dba)_3/PPh_3$ in toluene/DMF (10:1, v/v) at 115 °C.

polymers, PDPPTT-2T and PDPPMT-2T (Scheme 1), possess a high molecular weight (>100 kg mol^{-1}) and small bandgap, and show good solubility in toluene, but at the same time afford highly crystalline thin films. Processing either of the two polymers from toluene with diphenyl ether (DPE) as additive provides bottom gate–bottom contact (BGBC) configuration FETs with a hole mobility as high as 12.5 cm^2 V^{-1} s^{-1}. In addition, PSCs based on the two polymers as electron donor, processed from a toluene/DPE solvent mixture, show PCEs of 6.5% with a photoresponse above 900 nm. The results demonstrate that incorporating structural asymmetry into the main chain via different aromatic substituents is an efficient strategy to achieve high-performance FETs and PSCs of DPP polymers using nonchlorinated solution-processing.

The synthetic procedures for the DPP monomers and polymers are presented in Scheme 1. Starting from the initial precursor, ethyl 5-oxo-2-(thiophen-2-yl)-4,5-dihydro-1*H*-pyrrole-3-carboxylate (**1**)[38] with thiophene as aromatic group, and using TT or MT based nitriles, the asymmetric DPP compounds **2** and **3** were prepared. After *N*-alkylation and bromination of **2** and **3**, the asymmetric dibromo-DPP monomers **4** and **5** were obtained. The polymers PDPPTT-2T and PDPPMT-2T were synthesized via Stille polymerization, in which a $Pd_2(dba)_3/PPh_3$ (1:4) catalyst and toluene/DMF (10:1) solvent mixture were applied to reduce the homo-coupling side reactions and achieve a high molecular weight.[39] Both polymers show good solubility in $CHCl_3$. The polymers are also soluble in toluene, but form gel-like structures in 10 min. at room temperature (Supporting Information, Table S1). This indicates that the two polymers are less soluble in toluene than in $CHCl_3$. The molecular weight of the two polymers was determined by gel permeation chromatography (GPC) with *o*-DCB as eluent at 140 °C, as shown in Figure S1 in the Supporting Information. Both polymers show a number-average molecular weight (M_n) above 100 kg mol^{-1} and PDI around 2, which is comparable to analogous symmetric DPP polymers such as PDPP3T,[13] PMDPP3T,[31] and P1.[32] It is to be noticed that for both polymers, the repeating units can have two possible structures as shown in Figure S2 and S3 in the Supporting Information. Density functional theory (DFT) calculations reveal that the two types show similar frontier energy levels and have a planar backbone with very small torsion angles. The high molecular weight and coplanar backbone are beneficial for charge transport in FETs and PSCs.

The two polymers show similar electronic absorption spectra in $CHCl_3$ solution and in thin films. The optical bandgaps (E_g) of PDPPTT-2T and PDPPMT-2T were 1.38 eV and 1.39 eV in chloroform solution (Figure S4, Supporting Information), and 1.36 eV and 1.34 eV in thin films (**Figure 1**). The optical bandgap is similar to that of symmetric DPP polymers.[13,31,32] The two polymers have the same reduction and oxidation potentials of –1.31 and 0.00 V versus ferrocene (Fc/Fc$^+$) respectively, as determined by cyclic voltammetry in *o*-DCB (Figure S5 and Table S2, Supporting Information).

The two DPP polymers were applied in FETs devices with a BGBC configuration. The silicon dioxide gate dielectric used was passivated with octadecyltrichlorosilane (OTS). The polymers were applied via spin coating from $CHCl_3$ or toluene solution without or with DPE as additive and thermally annealed for 2 h at 120 °C in vacuum. Initially, the hole mobilities of PDPPTT-2T and PDPPMT-2T spin coated from $CHCl_3$ solution were measured to be 2.06 and 5.22 cm^2 V^{-1} s^{-1} (**Table 1** and Figure S6, Supporting Information). The hole mobilities were slightly less (1.96 and 4.68 cm^2 V^{-1} s^{-1}) when the polymers were processed from toluene solution. When adding a small amount of high-boiling-point DPE as additive into toluene solution, the hole mobilities increased dramatically to 5.24 and 10.3 cm^2 V^{-1} s^{-1} for PDPPTT-2T and PDPPMT-2T, with a maximum mobility of 12.5 cm^2 V^{-1} s^{-1} for the latter (**Figure 2**, Table 1, and Figure S7, Supporting Information). To the best of our knowledge, this represents the highest hole mobility for polymer FETs fabricated from a nonchlorinated solvent. Interestingly, PDPPMT-2T with methylthiophene as bridge has a more than doubled hole mobility compared to PDPPTT-2T with fused TT as bridge. The two polymers also have good solubility in other nonchlorinated solvents, such as xylene and 1,2,4-trimethylbenzene (TMB). FETs devices based on thin

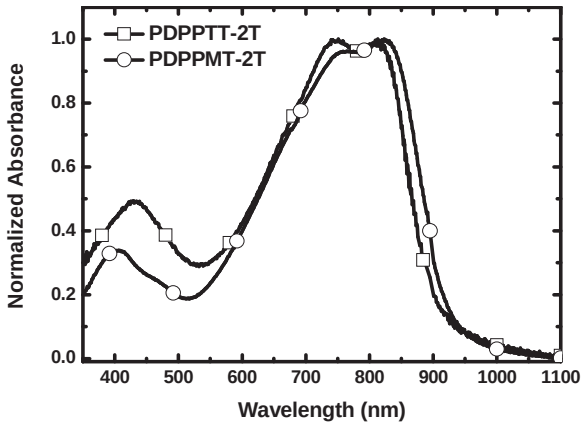

Figure 1. Absorption spectra of thin films of PDPPTT-2T and PDPPMT-2T.

films of the two polymers fabricated from xylene or TMB with or without DPE show similar hole mobilities compared to those from toluene solution (Figure S8,S9 and Table S3, Supporting Information).

The morphology and crystal characteristics of the DPP polymer films were further investigated by atomic force microscopy (AFM) image and 2D grazing-incidence wide-angle X-ray scattering (2D-GIWAXS), as shown in **Figure 3** and Figure S10 in the Supporting Information. The polymer films processed from toluene/DPE solutions show crystalline domains and possess a higher surface roughness (Figure S10c,d, Supporting Information) (2.13 and 1.38 nm for PDPPTT-2T and PDPP2T-T) than the films from toluene solution (Figure S10a,b, Supporting Information) (0.86 and 0.71 nm for PDPPTT-2T and PDPP2T-T). 2D-GIWAXS patterns show that the polymer films spin coated from toluene/DPE and annealed at 120 °C are highly ordered and highly crystalline, as evidenced by the series of reflections associated with the lamellar packing of the alkyl chains. Distinct (*h*00) diffraction peaks up to the fourth order can be observed in the out-of-plane direction (Figure 3a,b) for both polymers. The highest intensity (100) peaks of PDPPTT-2T and PDPPMT-2T at q_z = 0.30 and 0.34 Å^{-1} correspond *d*-spacings of 20.9 and 18.5 nm, respectively (Figure 3c,d and Table S4, Supporting Information). The distinct (010) diffraction peak in the in-plane direction of the PDPPTT-2T evidences π–π stacking (spacing: ca. 3.63 Å). PDPPMT-2T shows a less pronounced (010) diffraction peak also in the in-plane direction with a π–π stacking distance of ca. 3.9 Å and a low-intensity (100) peak can also be observed. This indicates that PDPPMT-2T has less preferential order than PDPPTT-2T, although PDPPMT-2T shows a much higher hole mobility than PDPPTT-2T. High mobilities for less-ordered organic semiconductors have also been reported in other high-molecular-weight conjugated polymers.[21,40] Semicrystalline conjugated polymers contain ordered and disordered regions in thin films. For high-mobility polymers it has been suggested that charge transport is predominantly occurring along the backbone and requires only occasional intermolecular hopping through short π-stacking bridges such that short-range intermolecular aggregation is sufficient for efficient long-range charge transport.[41,42] Compared to PDPPTT-2T, PDPPMT-2T may show better aggregation in the disordered regions, explaining the higher mobility.

The two polymers exhibit both (100) and (010) diffraction peaks in the out-of-plane direction when processed from toluene solution. We attribute this to the absence of a clear preference for edge on orientation of the polymer chains on the surface (Figure S11, Supporting Information). AFM and 2D-GIWAXS results shows that the polymer films fabricated from pure toluene solution exhibit less crystallinity and preferential orientation, which is consistent with their lower mobilities compared to films fabricated from toluene/DPE solutions. The 2D-GIWAXS results show that both asymmetric DPP polymers exhibit preferentially edge-on molecular packing with high crystallinity when processed from toluene/DPE solutions, which could lead to their high hole mobilities for in plane transport.

The two polymers were further applied as electron donors in bulk heterojunction photovoltaic cells after blending with phenyl-C_{71}-butyric acid methyl ester ([70]PCBM) as electron acceptor in an inverted device configuration with an ITO/ZnO electrode for electron collection and a MoO_3/Ag electrode for hole collection. The photoactive layers were carefully optimized with respect to the solvent used for spin coating, solvent additive, ratio of donor to acceptor, and thickness, as summarized in Table S5–S8 and Figure S12–S14 in the Supporting Information. The optimized polymer–fullerene weight ratio is 1:2. The *J*–*V* characteristics and external quantum efficiency (EQE) for the optimized solar cells are shown in **Figure 4**a,b and **Table 2**. The J_{sc}s were determined by integrating the EQE with the AM1.5G spectrum. PDPPTT-2T:[70]PCBM cells had a PCE of 5.1% with J_{sc} = 13.5 mA cm^{-2}, V_{oc} = 0.61 V, and fill factor (FF) = 0.63 when the active layer is spin coated from $CHCl_3$ with 10% *o*-DCB as additive. The PCE increased to 6.1% due to

Table 1. Field-effect hole mobilities of the DPP polymers in a BGBC configuration. The polymer thin films were thermally annealed at 120 °C for 2 h before measurement.

Polymer	Solvent	μ_h [cm^2 V^{-1} s^{-1}]		V_T	I_{on}/I_{off}
		Ave	Max	[V]	
PDPPTT-2T	$CHCl_3$	2.06	2.17	−10.8	1×10^7
	Toluene	1.96	2.07	−5.2	8×10^6
	Toluene/DPE (3%)	5.24	5.87	−7.5	2×10^5
PDPPMT-2T	$CHCl_3$	5.22	5.28	−1.7	4×10^4
	Toluene	4.68	4.87	−4.6	9×10^5
	Toluene/DPE (2%)	10.3	12.5	−2.9	7×10^4

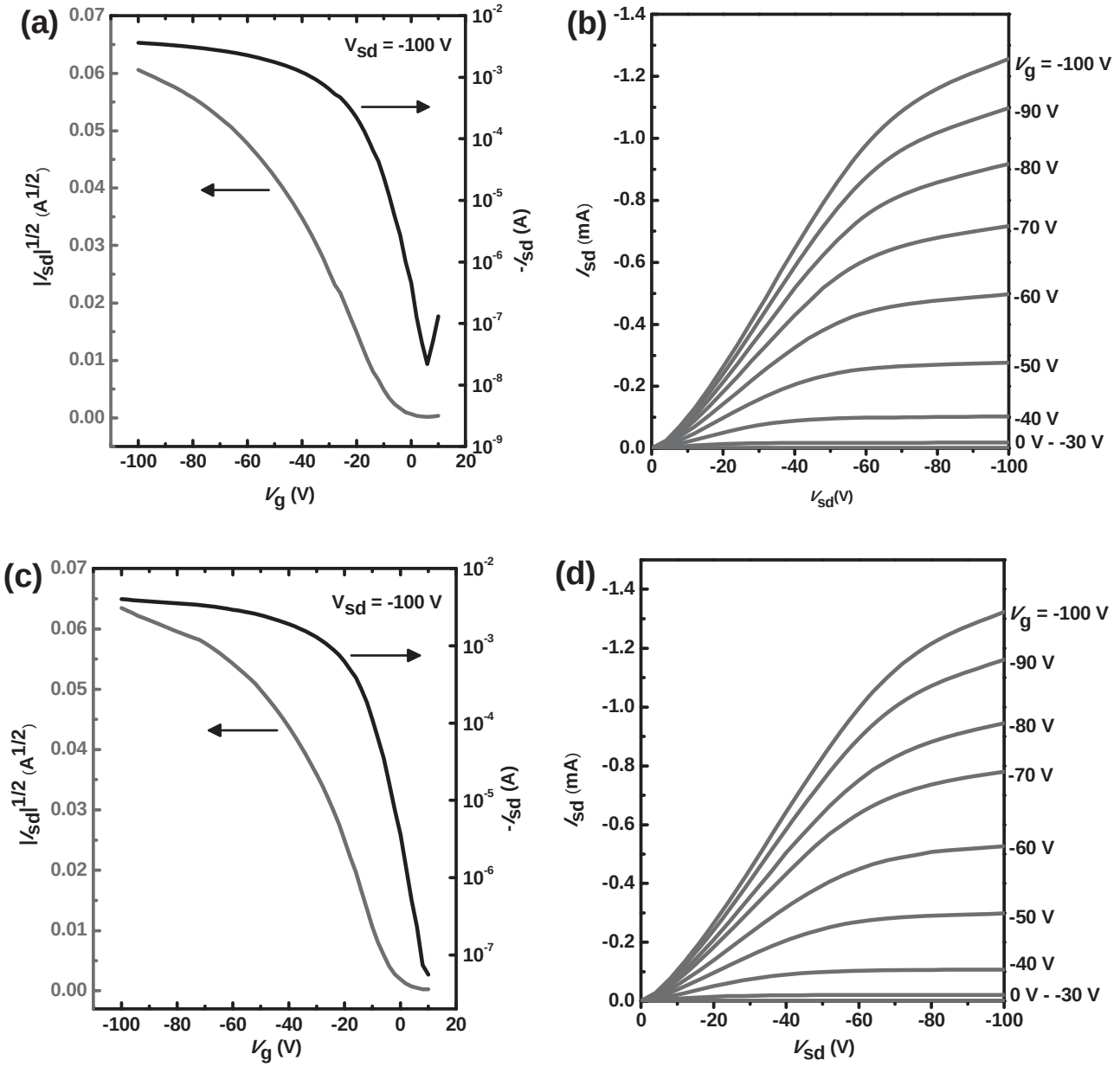

Figure 2. a,c) Transfer and b,d) output curves obtained from BGBC FET devices with DPP polymer thin films annealed at 120 °C: a,b) for PDPPTT-2T; c,d) for PDPPMT-2T. The thin films were spin cast from toluene/DPE solution.

much higher J_{sc} = 15.8 mA cm^{-2} when using toluene with 3% DPE as additive. For PDPPMT-2T:[70]PCBM cells, the PCE was 5.8% by using $CHCl_3$ with 2% DPE as additive, which increased to 6.5% when spin coating from toluene/DPE. This was mainly due to the enhancement of J_{sc} from 15.1 to 15.8 mA cm^{-2} and FF from 0.61 to 0.66. The two cells processed from toluene/DPE solution show a broad photoresponse from 300 nm to 900 nm with a maximum EQE over 0.55 in the near-infrared spectral region where the polymer absorbs light (Figure 4b). The photo-active layers can also be fabricated from nonchlorinated xylene or TMB solutions with DPE as additive, which gave comparable PCEs as films fabricated from toluene/DPE system (Table S9 and Figure S15, Supporting Information).

The photoactive layers were further investigated by 2D-GWAXS and transmission electron microscopy (TEM). Clear (100) and (200) diffraction peaks can be observed in out-of-plane direction, but the higher order diffraction peaks are no longer visible in the blend (Figure 4c,d, and Figure S16, Supporting Information). This indicates that the crystallinity of DPP polymers is reduced in the blends with [70]PCBM compared to the pure films. Accordingly, the diffraction (010) peak in the blend films can be found in out-of-plane direction but with low intensity. The diffraction halo observed near q = 1.32 Å^{-1} is attributed to [70]PCBM. TEM images based on the polymer–fullerene systems spin coated from toluene/DPE solution reveal that both of PDPPTT-2T and PDPPMT-2T

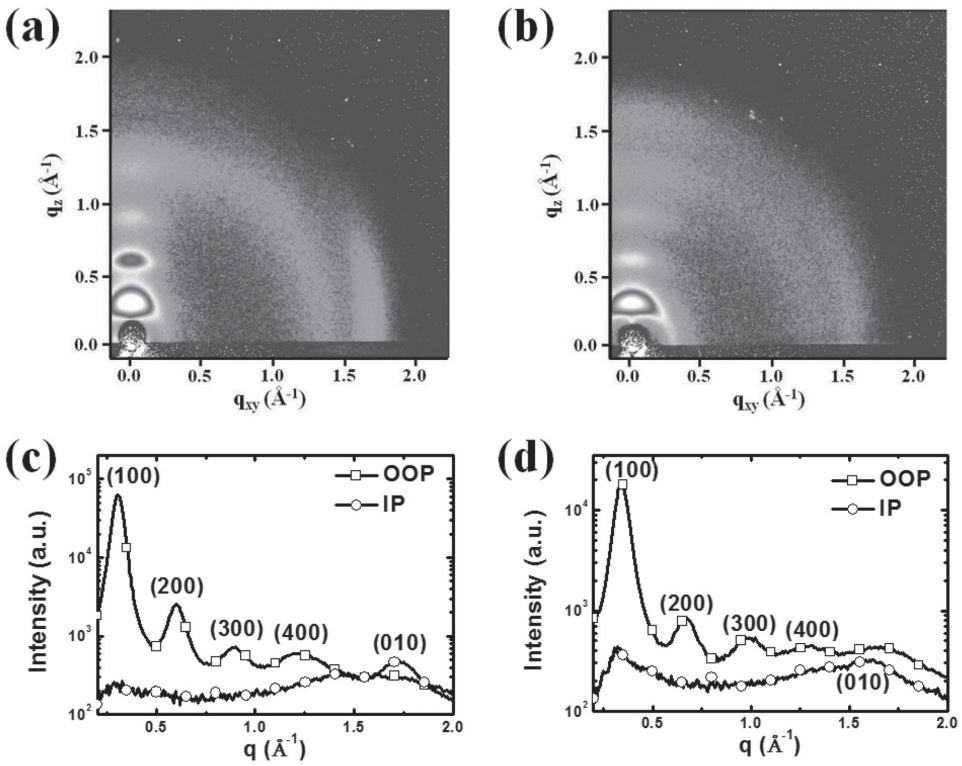

Figure 3. Characteristics of the polymer thin films spin coated from toluene/DPE and annealed at 120 °C. a,b) 2D-GIWAXS patterns, and c,d) the out-of-plane (OOP) and in-plane (IP) cuts of the corresponding 2D-GIWAXS patterns: a,c) for PDPPTT-2T; b,d) for PDPPMT-2T.

present fibril-like nanostructures with a diameter below 10 nm, similar to other DPP-fullerene blend films.[19] Because the radius of these polymer fibrils is on the order of the exciton diffusion length, most excitons will reach the donor/acceptor interface to generate charges and improve the PCE.

Interestingly, solar cells fabricated from toluene/DPE exhibit higher J_{sc}s, FFs, and PCEs than those from $CHCl_3$ with *o*-DCB or DPE as additive, which may originate from the morphology difference in blend films. AFM results show that polymer:[70]PCBM films fabricated from toluene/DPE solution have a higher RMS roughness than films from $CHCl_3$ solution (Figure S17, Supporting Information), indicating more micro-phase separation in blend films. 2D-GIWAXS results also reveal that the blend films spin coated from toluene/DPE have strong (100) diffraction peaks (Figure 4c,d) as compared to those spin coated from $CHCl_3$ mixture solution (Figure S18a–d, Supporting Information), which confirms that the polymers in blend films spin coated from toluene/DPE have improved aggregation and crystallinity. Further analysis by TEM shows that the blend films fabricated from $CHCl_3$ with additive contain large fibril-like structures (PDPPTT-2T) (Figure S18e, Supporting Information) or less-detectable fibers (PDPPMT-2T) (Figure S19f, Supporting Information), both of which is not beneficial for charge generation. As indicated in the solubility test, the polymers form gel-like structures in toluene solution, indicating pre-aggregation before solution-processing. This may responsible for the better aggregation of polymers in blending films and achieve high PCEs when solution-processed from toluene/DPE.

In conclusion, two asymmetric DPP polymers with different aromatic substituents were designed, synthesized, and applied in FETs and PSCs. The new polymers provide high molecular weights, small bandgaps, and good solubility in toluene. The polymers have hole mobilities as high as 12.5 $cm^2\ V^{-1}\ s^{-1}$ in FETs due to their high crystallinity in thin films when processed from toluene/DPE solution. With the same solvent combination, photovoltaic devices based on these two polymers reach PCEs of 6.5% with a photoresponse up to 900 nm. The results demonstrate that DPP polymers that have an asymmetry in the flanking aromatic substituents form a successful approach toward semiconducting materials that can be processed from nonchlorinated solvents, while maintaining a high performance in FETs and PSCs.

Experimental Section

The organic FETs were fabricated on a commercial $Si/SiO_2/Au$ substrate purchased from First MEMS Co. Ltd. A heavily N-doped Si wafer with an SiO_2 layer of 300 nm served as the gate electrode and dielectric layer, respectively. The Ti (2 nm)/Au (28 nm) source–drain electrodes were sputtered and patterned by a lift-off technique. Before deposition of the organic semiconductor, the gate dielectrics were treated with OTS in a vacuum oven at a temperature of 120 °C, forming an OTS self-assembled monolayers. The treated substrates were rinsed successively with hexane, chloroform, and isopropyl alcohol. Polymer thin films were spin coated on the substrate from solution with a thickness of around 30–50 nm. The devices were thermally annealed at 120 °C in a high-vacuum chamber (ca. 10^{-3} Pa) for 2 h, cooled down, and then moved into a glove box filled with N_2. The devices were measured on a Keithley

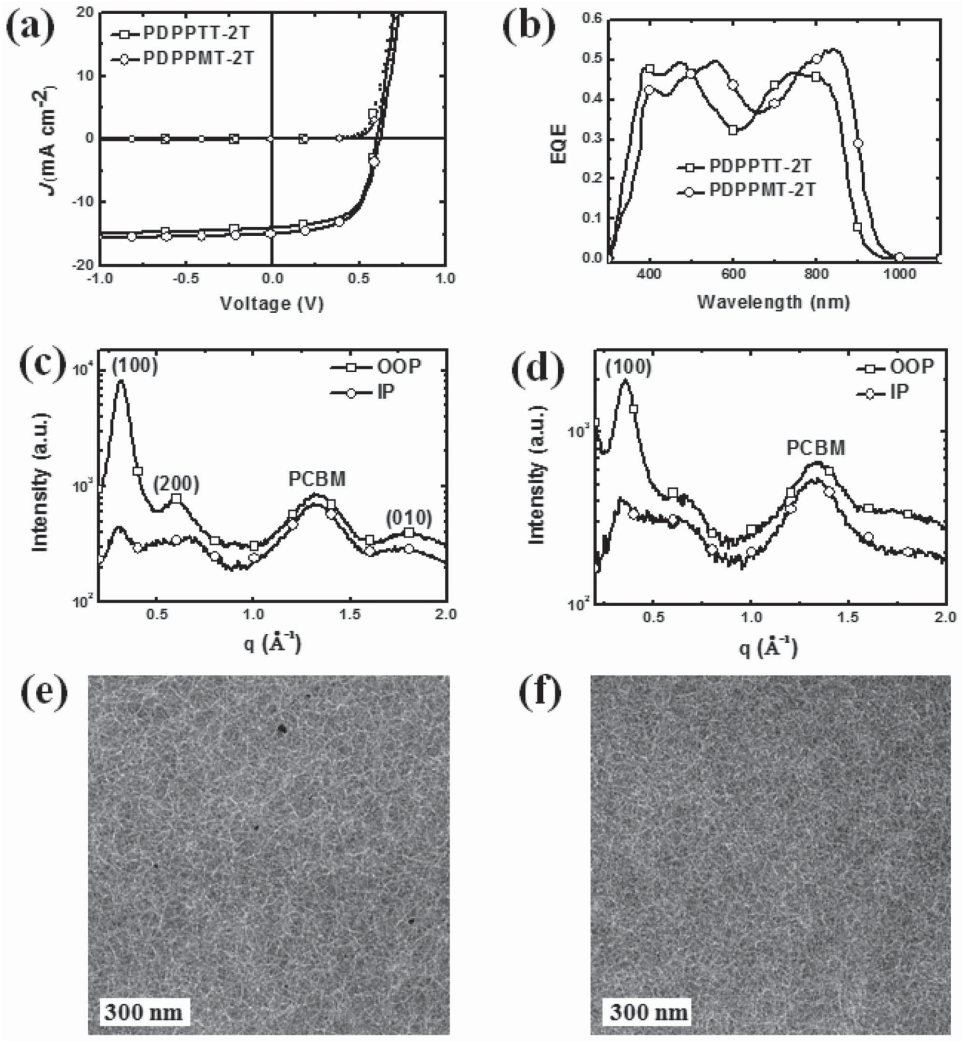

Figure 4. a) *J*–*V* characteristics in dark (dashed lines) and under white light illumination (solid lines). b) EQE of the optimized polymer:[70]PCBM (1:2) solar cells fabricated from toluene/DPE solution. c) The out-of-plane (OOP) and in-plane (IP) line cuts of the 2D GIWAXS patterns of optimized PDPPTT-2T:[70]PCBM (1:2) thin films fabricated from toluene/DPE solution. d) Same for PDPPMT-2T:[70]PCBM (1:2). e) Bright-field TEM image (1.2 μm × 1.2 μm) of the optimized PDPPTT-2T:[70]PCBM (1:2) thin films fabricated from toluene/DPE solution. f) Same for DPPMT-2T:[70]PCBM (1:2).

4200 SCS semiconductor parameter analyzer at room temperature. The mobilities were calculated from the saturation region with the following equation: $I_{DS} = (W/2L)C_i\mu(V_G - V_T)^2$, where I_{SD} is the drain–source current, W is the channel width (1400 μm), L is the channel length (30 μm for PDPPTT-2T and 40 μm for PDPPMT-2T), μ is the field-effect mobility, C_i is the capacitance per unit area of the gate dielectric layer, and V_G and V_T are the gate voltage and threshold voltage, respectively. This equation defines the important characteristics of electron mobility (μ), on/off ratio (I_{on}/I_{off}), and threshold voltage (V_T), which could be deduced by the equation from the plot of current–voltage.

Photovoltaic devices with inverted configuration were made by spin coating a ZnO sol–gel[43] at 4000 rpm for 60 s onto precleaned, patterned ITO substrates. The photoactive layer was deposited by spin coating a chloroform (or toluene) solution containing DPP polymers and [70]PCBM and the appropriate amount of processing additive such as DIO, o-DCB, or DPE in air. MoO_3 (10 nm) and Ag (100 nm)

Table 2. Characteristics of optimized inverted solar cells of the DPP polymers with [70]PCBM.

Polymer	Solvent	Thickness [nm]	J_{sc}[a)] [mA cm^{-2}]	V_{oc} [V]	FF	PCE [%]
PDPPTT-2T[b)]	$CHCl_3$/*o*-DCB (10%)	100	13.5	0.61	0.63	5.1
	Toluene/DPE (3%)	90	15.8	0.60	0.64	6.1
PDPPMT-2T[b)]	$CHCl_3$/DPE (2%)	70	15.1	0.63	0.61	5.8
	Toluene/DPE (2%)	65	15.8	0.62	0.66	6.5

[a)]J_{sc} as calculated by integrating the EQE spectrum with the AM1.5G spectrum; [b)]Weight ratio of the polymers to [70]PCBM is 1:2.

were deposited by vacuum evaporation at ca. 4×10^{-5} Pa as the back electrode.

The active area of the cells was 0.04 cm^2. The *J–V* characteristics were measured by a Keithley 2400 source meter unit under AM1.5G spectrum from a solar simulator (Enlitech model SS-F5–3A). Solar simulator illumination intensity was determined at 100 mW cm^{-2} using a monocrystal silicon reference cell with KG5 filter. Short-circuit currents under AM1.5G conditions were estimated from the spectral response and convolution with the solar spectrum. The EQE was measured by a Solar Cell Spectral Response Measurement System QE-R3011 (Enli Technology Co., Ltd.). The thickness of the active layers in the photovoltaic devices was measured on a Veeco Dektak XT profilometer.

TEM was performed on a Tecnai G^2 Sphera transmission electron microscope (FEI) operated at 200 kV. 2D-GIWAXS measurements were conducted on a Xenocs-SAXS/WAXS system with X-ray wavelength of 1.5418 Å. The film samples were irradiated at a fixed angle of 0.2°. All film samples were prepared by spin coating toluene/DPE solutions on Si substrates. The pure polymer thin films were annealed at 120 °C for 10 min before measurement.

Supporting Information

Supporting Information is available from the Wiley Online Library or from the author.

Acknowledgements

Y.J., C.X., and Q.W. contributed equally to this work. The authors thank Ralf Bovee at Eindhoven University of Technology (TU/e, Netherlands) for GPC analysis and Jacobus J. van Franeker (TU/e) for TEM measurements. This work was supported by the Recruitment Program of Global Youth Experts of China. The work of Q.W. forms part of the research program of the Dutch Polymer Institute (DPI), project #762. The work was further supported by the National Natural Science Foundation of China (21574138, 21474026), the 973 Program (2011CB932301, 2014CB643600, 2013CB933500), and the Strategic Priority Research Program (XDB12010100) of the Chinese Academy of Sciences. The research forms part of the Solliance OPV program and has received funding from the Ministry of Education, Culture and Science (Gravity program 024.001.035) of the Netherlands.

Received: August 31, 2015
Revised: October 5, 2015
Published online: November 30, 2015

[1] Z. Yi, S. Wang, Y. Liu, *Adv. Mater.* **2015**, *27*, 3589.
[2] C. B. Nielsen, M. Turbiez, I. McCulloch, *Adv. Mater.* **2013**, *25*, 1859.
[3] B. Sun, W. Hong, Z. Yan, H. Aziz, Y. Li, *Adv. Mater.* **2014**, *26*, 2636.
[4] J. Y. Back, H. Yu, I. Song, I. Kang, H. Ahn, T. J. Shin, S.-K. Kwon, J. H. Oh, Y.-H. Kim, *Chem. Mater.* **2015**, *27*, 1732.
[5] H.-J. Yun, S.-J. Kang, Y. Xu, S. O. Kim, Y.-H. Kim, Y.-Y. Noh, S.-K. Kwon, *Adv. Mater.* **2014**, *26*, 7300.
[6] I. Kang, H.-J. Yun, D. S. Chung, S.-K. Kwon, Y.-H. Kim, *J. Am. Chem. Soc.* **2013**, *135*, 14896.
[7] H. J. Chen, Y. L. Guo, G. Yu, Y. Zhao, J. Zhang, D. Gao, H. T. Liu, Y. Q. Liu, *Adv. Mater.* **2012**, *24*, 4618.
[8] J. S. Ha, K. H. Kim, D. H. Choi, *J. Am. Chem. Soc.* **2011**, *133*, 10364.
[9] E. Zhou, J. Cong, K. Hashimoto, K. Tajima, *Energy Environ. Sci.* **2012**, *5*, 9756.
[10] K. H. Hendriks, W. Li, M. M. Wienk, R. A. J. Janssen, *J. Am. Chem. Soc.* **2014**, *136*, 12130.
[11] H. Choi, S.-J. Ko, T. Kim, P.-O. Morin, B. Walker, B. H. Lee, M. Leclerc, J. Y. Kim, A. J. Heeger, *Adv. Mater.* **2015**, *27*, 3318.
[12] R. S. Ashraf, I. Meager, M. Nikolka, M. Kirkus, M. Planells, B. C. Schroeder, S. Holliday, M. Hurhangee, C. B. Nielsen, H. Sirringhaus, I. McCulloch, *J. Am. Chem. Soc.* **2014**, *137*, 1314.
[13] K. H. Hendriks, G. H. L. Heintges, V. S. Gevaerts, M. M. Wienk, R. A. J. Janssen, *Angew. Chem., Int. Ed.* **2013**, *52*, 8341.
[14] R. Po, G. Bianchi, C. Carbonera, A. Pellegrino, *Macromolecules* **2015**, *48*, 453.
[15] A. C. Rochat, L. Cassar, A Iqbal, *EP 94911*, **1983**.
[16] A. T. Yiu, P. M. Beaujuge, O. P. Lee, C. H. Woo, M. F. Toney, J. M. J. Fréchet, *J. Am. Chem. Soc.* **2012**, *134*, 2180.
[17] I. Meager, R. S. Ashraf, S. Rossbauer, H. Bronstein, J. E. Donaghey, J. Marshall, B. C. Schroeder, M. Heeney, T. D. Anthopoulos, I. McCulloch, *Macromolecules* **2013**, *46*, 5961.
[18] W. Li, K. H. Hendriks, A. Furlan, W. S. C. Roelofs, S. C. J. Meskers, M. M. Wienk, R. A. J. Janssen, *Adv. Mater.* **2014**, *26*, 1565.
[19] W. Li, K. H. Hendriks, A. Furlan, W. S. C. Roelofs, M. M. Wienk, R. A. J. Janssen, *J. Am. Chem. Soc.* **2013**, *135*, 18942.
[20] H.-J. Yun, G. B. Lee, D. S. Chung, Y.-H. Kim, S.-K. Kwon, *Adv. Mater.* **2014**, *26*, 6612.
[21] H.-J. Yun, J. Cho, D. S. Chung, Y.-H. Kim, S.-K. Kwon, *Macromolecules* **2014**, *47*, 7030.
[22] H. H. Choi, J. Y. Baek, E. Song, B. Kang, K. Cho, S.-K. Kwon, Y.-H. Kim, *Adv. Mater.* **2015**, *27*, 3626.
[23] W. K. Chan, Y. Chen, Z. Peng, L. Yu, *J. Am. Chem. Soc.* **1993**, *115*, 11735.
[24] B. Tieke, A. R. Rabindranath, K. Zhang, Y. Zhu, *Beilstein J. Org. Chem.* **2010**, *6*, 830.
[25] J. W. Jung, F. Liu, T. P. Russell, W. H. Jo, *Chem. Commun.* **2013**, *49*, 8495.
[26] X. Zhang, C. Xiao, A. Zhang, F. Yang, H. Dong, Z. Wang, X. Zhan, W. Li, W. Hu, *Polym. Chem.* **2015**, *6*, 4775.
[27] M. M. Wienk, M. Turbiez, J. Gilot, R. A. J. Janssen, *Adv. Mater.* **2008**, *20*, 2556.
[28] J. C. Bijleveld, A. P. Zoombelt, S. G. J. Mathijssen, M. M. Wienk, M. Turbiez, D. M. de Leeuw, R. A. J. Janssen, *J. Am. Chem. Soc.* **2009**, *131*, 16616.
[29] C. H. Woo, P. M. Beaujuge, T. W. Holcombe, O. P. Lee, J. M. J. Fréchet, *J. Am. Chem. Soc.* **2010**, *132*, 15547.
[30] M. S. Chen, O. P. Lee, J. R. Niskala, A. T. Yiu, C. J. Tassone, K. Schmidt, P. M. Beaujuge, S. S. Onishi, M. F. Toney, A. Zettl, J. M. J. Fréchet, *J. Am. Chem. Soc.* **2013**, *135*, 19229.
[31] W. Li, A. Furlan, K. H. Hendriks, M. M. Wienk, R. A. J. Janssen, *J. Am. Chem. Soc.* **2013**, *135*, 5529.
[32] H. Bronstein, Z. Chen, R. S. Ashraf, W. Zhang, J. Du, J. R. Durrant, P. Shakya Tuladhar, K. Song, S. E. Watkins, Y. Geerts, M. M. Wienk, R. A. J. Janssen, T. Anthopoulos, H. Sirringhaus, M. Heeney, I. McCulloch, *J. Am. Chem. Soc.* **2011**, *133*, 3272.
[33] L. Dou, W.-H. Chang, J. Gao, C.-C. Chen, J. You, Y. Yang, *Adv. Mater.* **2013**, *25*, 825.
[34] B. Carsten, J. M. Szarko, L. Lu, H. J. Son, F. He, Y. Y. Botros, L. X. Chen, L. Yu, *Macromolecules* **2012**, *45*, 6390.
[35] W. Li, W. S. C. Roelofs, M. Turbiez, M. M. Wienk, R. A. J. Janssen, *Adv. Mater.* **2014**, *26*, 3304.
[36] T. W. Holcombe, J.-H. Yum, Y. Kim, K. Rakstys, M. Grätzel, *J. Mater. Chem. A* **2013**, *1*, 13978.
[37] J.-H. Huang, K.-J. Jiang, F. Zhang, W. Wu, S.-G. Li, L.-M. Yang, Y.-L. Song, *RSC Adv.* **2014**, *4*, 16906.
[38] T. Aysha, S. Luňák Jr., A. Lyčka, J. Vyňuchal, Z. Eliáš, A. Růžička, Z. Padělková, R. Hrdina, *Dyes Pigm.* **2013**, *98*, 530.
[39] K. H. Hendriks, W. Li, G. H. L. Heintges, G. W. P. van Pruissen, M. M. Wienk, R. A. J. Janssen, *J. Am. Chem. Soc.* **2014**, *136*, 11128.

[40] H. Bronstein, Z. Chen, R. S. Ashraf, W. Zhang, J. Du, J. R. Durrant, P. Shakya Tuladhar, K. Song, S. E. Watkins, Y. Geerts, M. M. Wienk, R. A. J. Janssen, T. Anthopoulos, H. Sirringhaus, M. Heeney, I. McCulloch, *J. Am. Chem. Soc.* **2011**, *133*, 3272.
[41] X. Zhang, H. Bronstein, A. J. Kronemeijer, J. Smith, Y. Kim, R. J. Kline, L. J. Richter, T. D. Anthopoulos, H. Sirringhaus, K. Song, M. Heeney, W. Zhang, I. McCulloch, D. M. DeLongchamp, *Nat. Commun.* **2013**, *4*, 2238.
[42] R. Noriega, J. Rivnay, K. Vandewal, F. P. V. Koch, N. Stingelin, P. Smith, M. F. Toney, A. Salleo, *Nat. Mater.* **2013**, *12*, 1038.
[43] Y. M. Sun, J. H. Seo, C. J. Takacs, J. Seifter, A. J. Heeger, *Adv. Mater.* **2011**, *23*, 1679.